Available online at www.sciencedirect.com
ScienceDirect
Journal of Nuclear Materials 361 (2007) 282–288
journal of nuclear materials
www.elsevier.com/locate/jnucmat

The radiation damage database: Section on helium cross section

W. Lu *, M.S. Wechsler

Department of Nuclear Engineering, North Carolina State University, Raleigh, NC 27695-7909, USA

Abstract

A radiation damage database with emphasis on spallation interactions is described. Currently, the database contains damage energy, displacement, helium, and hydrogen cross sections for 23 elemental targets irradiated by proton and neutron projectiles up to 3.2 GeV. In this paper, the focus is on proton-induced helium cross sections, but it is shown that for high energies (above about 500 MeV) proton- and neutron-induced helium cross sections are almost equal. The cross section calculations were run on the Cascade–Exciton Model code (no options) and also on the Bertini code with three nuclear level-density models and multistage pre-equilibrium model on and off. Calculation and experimental results are compared. For various targets, we tried to determine which code and options give best agreement with experiment. In some cases, such determinations are uncertain, partly because of limited and conflicting experimental information and partly perhaps because of the need for modifications in the codes.

PACS: 24.10.Lx; 61.80.−x; 61.80.Az; 61.80.Bg; 61.80.Hg; 61.80.Jh

1. Introduction

In recent years, accelerator-driven spallation sources have aroused great interest in materials research, life sciences and transmutation of nuclear wastes. The design and construction of such accelerator-driven facilities impose new challenges to the target and structural materials regarding their ability to withstand radiation damage in a spallation radiation spectrum. The accelerator-driven facility is usually propelled by high-energy protons in 1 GeV range. At such high energies, the incident proton can interact with individual nucleons inside the struck nucleus, producing abundant high-energy protons and spallation neutrons. Compared to that in the fission or fusion spectrum, radiation damage to materials in the spallation spectrum is more severe due to the added displacements and the new particles produced, mainly helium and hydrogen for the light particles [1].

Although it is essential to evaluate the radiation damage by high-energy protons and neutrons for the spallation facilities, the calculation of radiation damage (mainly the production of displacements, helium and hydrogen) is often inconsistent and discrepant due to the various models and codes used. The object of the NCSU (North Carolina State University) Radiation Damage Database (the Database) is, therefore, to assist in establishing a standard method for calculating spallation damage

* Corresponding author. Present address: Bldg. 8600, MS 6460, Spallation Neutron Source Project, Oak Ridge National Laboratory, Oak Ridge, TN 37831, USA. Tel.: +1 865 241 9603; fax: +1 865 574 6080.
E-mail address: luw2@ornl.gov (W. Lu).

0022-3115/$ - see front matter © 2006 Elsevier B.V. All rights reserved.
doi:10.1016/j.jnucmat.2006.12.005

that meets with reasonably widespread acceptance. The Database would hope to be an accurate and comprehensive cross section library, incorporating a referenced variety of radiation-transport codes for calculation, evaluated cross section values, and experimental results for benchmarking. The main content of the Database, cross sections for damage energy, displacements, helium and hydrogen production, is, to a large extent, completed. The design of a friendly interface for convenient use of the Database is underway. Damage energy and displacement cross sections are already discussed in [2,3], and the focus of this paper is on helium production cross sections for proton energies from 1 MeV to 3.2 GeV and neutron energies from 1E−8 MeV to 3.2 GeV.

2. The NCSU radiation damage database

The radiation damage database contains damage energy, displacement, helium, hydrogen, and transmutation production cross sections useful for spallation radiation damage calculations. It includes 23 elemental targets and 8 alloys, most of which are commonly used materials subjected to radiation at a spallation facility, as listed below:

Target elements
- Group 1: $_{12}$Mg, $_{13}$Al, $_{14}$Si
- Group 2: $_{22}$Ti, $_{23}$V, $_{24}$Cr, $_{25}$Mn, $_{26}$Fe, $_{27}$Co, $_{28}$Ni, $_{29}$Cu
- Group 3: $_{40}$Zr, $_{41}$Nb, $_{42}$Mo, $_{47}$Ag, $_{50}$Sn
- Group 4: $_{73}$Ta, $_{74}$W, $_{79}$Au, $_{80}$Hg, $_{82}$Pb, $_{83}$Bi
- Group 5: $_{92}$U

Target alloys (compositions used in the calculations given in at.%):
- AlMg3 (Al–2.72Mg–0.35Mn–0.25Fe)
- EP823 (Fe–12Cr–1.8Si–0.9Ni–0.7Mo–0.7Mn)
- Eurofer97 (Fe–9Cr–1.1W–0.4Mn)
- F82H (Fe–7.9Cr–2.0W–0.2V)
- HT9 (Fe–11.8Cr–1.0Mo–0.6Ni–0.5Mn)
- SS316L (Fe–17.5Cr–12.2Ni–2.5Mo–1.8Mn)
- T91 (Fe–8.6Cr–1.0Mn–0.2Ni)
- Zr-2 (Zr–1.36Sn–0.17Fe–0.13O–0.11Cr–0.07Ni)

As can be seen, the 23 targets are divided into five groups, according to their atomic masses and the cross section patterns that they exhibit. The targets in the same group show similar characteristics in the evaluation of the cross sections.

The high-energy proton and neutron cross sections ($E > 150$ MeV) in the Database are calculated by intranuclear cascade (INC) models: Bertini [4,5], ISABEL [6] and CEM2k (version of the Cascade–Exciton Model in year 2000) [7,8]. We refer to calculations using these INC models as 'high-energy calculations.' Typically, we ran 10^6 histories for each cross section determination for the Bertini and ISABEL INC calculations and 10^5 histories for CEM2k. We use the term 'low-energy calculations' for energies below 150 MeV, where the INC models are believed to be inaccurate. For the low-energy cross sections, values from SPECTER [9], ENDF-6 (Evaluated Nuclear Data Formats) [10] ($E < 20$ MeV, for neutrons) and LA150 [11] ($20 < E < 150$ MeV for neutrons; $1 < E < 150$ MeV for protons) are adopted in the Database. The SPECTER information refers to neutron radiation damage only, and the nuclear reaction data in SPECTER were obtained from ENDF/B-5. Table 1 shows which sources were used in developing the Database, depending upon the projectile, type of cross section, and projectile energy. As for proton-induced damage energy and displacement cross sections at low energies, the contribution of the elastic scattering is not fully implemented in INC models. Neither is it included in the evaluated cross section sources mentioned above which actually have no proton-induced damage energy or displacement cross sections at all. This gap is now filled in

Table 1
Cross section sources for the NCSU radiation damage database

Projectile	Cross section Type[a]	Energy range $E < 20$ MeV	Energy range $20 < E < 150$ MeV	Energy range $150 < E < 3200$ MeV
n	DECS, DCS	ENDF, SPECTER	LA150	High-energy calc'n
n	HeCS, HCS	ENDF, SPECTER	LA150	High-energy calc'n
p	DECS, DCS	SRIM	High-energy calc'n	High-energy calc'n
p	HeCS, HCS	LA150	LA150	High-energy calc'n

[a] DECS, DCS, HeCS and HCS are, respectively, damage energy cross section, displacement cross section, helium cross section and hydrogen cross section.

the Database with the calculations [3] using SRIM (stopping and range of ions in matter) [12]. Cross sections are reported in SRIM up to 2 GeV, but since no account is taken of intranuclear cascades and spallation, we include SRIM among the low-energy sources. For Bertini and ISABEL models, three different level densities, GCCI (Gilbert–Cameron–Cook–Ignatyuk level density) [13–15], HETC (High-Energy Nucleon–Meson Transport Code) [16] and Jülich [17] with and without the multistage pre-equilibrium model (MPM) [18], are used for calculating helium and hydrogen cross sections. The high-energy cross sections are either benchmarked by experimental results (helium and hydrogen cross sections) or analyzed as to how good a match is made where they connect with low-energy values (damage energy and displacement cross sections [2,3]).

This paper presents the calculation and evaluation of helium cross sections by examining a typical target element from each group.

3. Proton-induced helium cross sections

The presence of helium and hydrogen in materials often causes them to become more brittle. Therefore, these products are an important consideration in radiation damage. The helium cross sections calculated by the default options of MCNPX [18], however, often lead to an unsatisfying disagreement with the experimental results. One example of such disagreement is shown by Dai et al. [19] in measuring helium production at the aluminum beam window of the SINQ target. It is one of the goals for the Database to help to resolve such disagreement.

As shown in Table 1, the helium cross sections at high energies are calculated by the high-energy INC-based models. Three INC models are included in the Database: Bertini, ISABEL and CEM2k. Compared to Bertini and ISABEL, CEM2k may be more validated because it was tested against some recent measurements [8]. Also, the cut-off energy from the intranuclear cascade in CEM2k is sufficiently low rather than about 7 MeV as in Bertini and ISABEL. But CEM2k has an inherent MPM and offers no option to remove the MPM in MCNPX. Bertini and ISABEL, on the other hand, can be configured with or without MPM. Furthermore, Bertini and ISABEL have an option for one of three nuclear level-density models: GCCI, HETC and Jülich. The level density is a way to describe the structure of a highly excited nucleus, which plays an important role in the formation of light particles including helium.

The proton-induced helium cross sections up to 3.2 GeV from Bertini with the three level densities and MPM on and off and from CEM2k are plotted in Figs. 1–5 for typical target elements in each group. As it only allows incident particle energy up to 1 GeV, the ISABEL model is not discussed further here for the helium cross section. It is obvious in Figs. 1–5 that cross section values in Bertini calculated with MPM on are lower than those with MPM off. This is because in the pre-equilibrium stage part of the energy is used to increase the

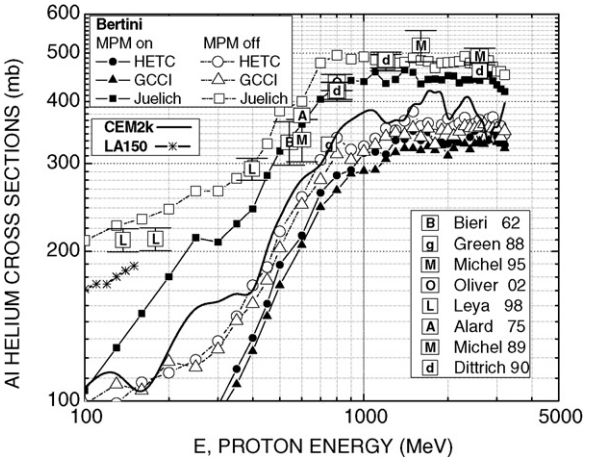

Fig. 1. Helium cross section versus proton energy for Al. High-energy calculations, experimental data and low-energy calculations (LA150).

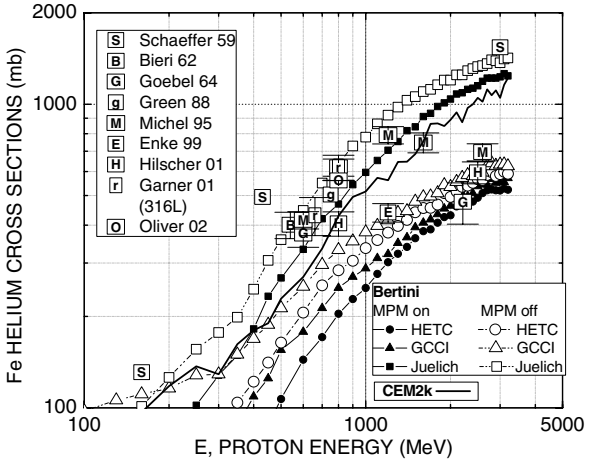

Fig. 2. Helium cross section versus proton energy for Fe. High-energy calculations and experimental data.

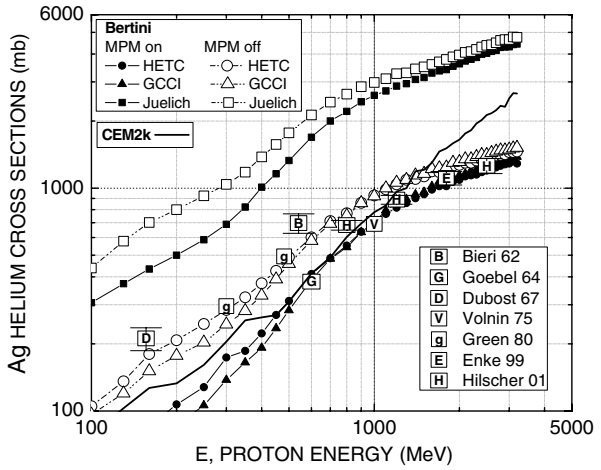

Fig. 3. Helium cross section versus proton energy for Ag. High-energy calculations and experimental data.

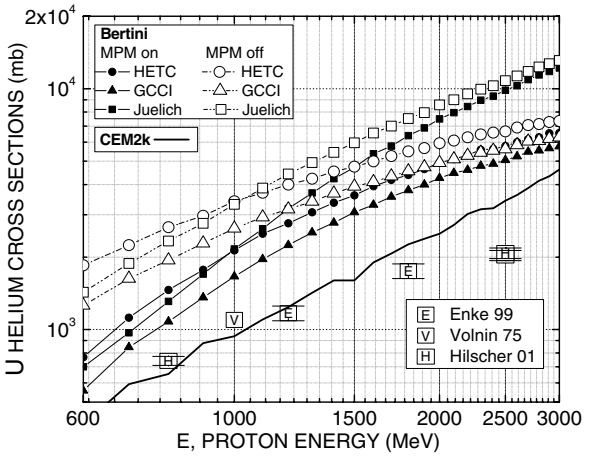

Fig. 5. Helium cross section versus proton energy for U. High-energy calculations and experimental data.

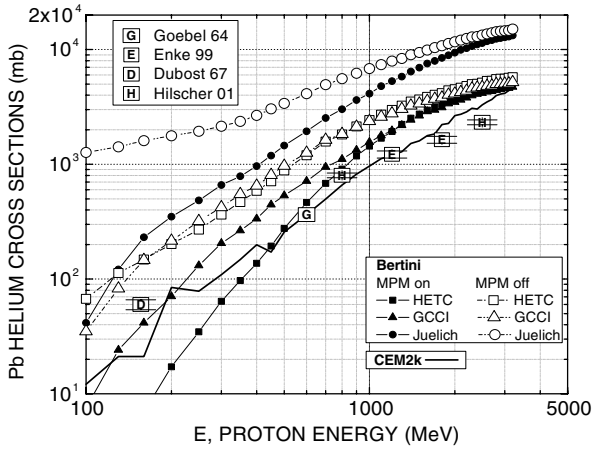

Fig. 4. Helium cross section versus proton energy for Pb. High-energy calculations and experimental data.

excitation number of the nucleus without producing light particles. The Jülich model shows consistently higher values than the other two level-density models. But the cross sections of GCCI and HETC are quite close to each other with HETC values slightly higher in Groups 1, 4, and 5 and GCCI values slightly higher in Groups 2 and 3. With increasing target mass, the cross sections of CEM2k move from between Jülich and GCCI/HETC to below GCCI/HETC.

The high-energy INC-calculated helium cross sections in Figs. 1–5 are plotted against experimental data [20–38]. The legends with square symbols (containing a single lower- or upper-case letter) give the first-named author and publication year for the experimental investigations. For the calculations, the differences due to the INC models and their configurations are thus examined to find the most realistic cross section data. Fig. 1 shows the experimental results and the high-energy calculated cross sections for Al representing Group 1, the lightest targets. Al is a typical structural material in a spallation facility. It is used for the proton beam window and target structure in SINQ and the pressure boundary of the inner reflector plug in SNS [39]. In Fig. 1, except for one point by Green et al. [23], the experimental data agree best with calculated Bertini values using the Jülich level-density model. CEM2k and the other two level-density models in Bertini underestimate the helium production. LA150 cross sections are also plotted in Fig. 1 (short segment at lower left below 150 MeV), which indicates a fairly good connection at 150 MeV to experimental cross sections due to Leya et al. [29]. Close examination indicates perhaps that Bertini–Jülich agrees better with MPM on than with MPM off. But it does not rule out the use of Bertini–Jülich with MPM off.

Group 2 contains nine light targets, among which Fe, Cr and Ni are the major constituents of stainless steel, an important structural and reflector material in a spallation facility. The situation in Fig. 2, which shows the experimental and high-energy INC-calculated cross sections for Fe, is complicated. The experimental data seem scattered among INC models and different level-density models. But they still fall within the upper and lower boundary of INC calculations. The data of Schaeffer and Zahringer

[20] provide the upper boundary of the experimental results and are closest to the results of Bertini–Jülich with MPM off, the upper boundary of the INC calculations. There is some doubt concerning the data of Michel et al. [24] since they show a decrease in helium cross section for proton energies above 1.2 GeV, which is unusual based on INC calculations and other experiments. Most of the experimental data are clustered around Bertini–Jülich curves with a few points falling into the Bertini–GCCI/HETC range. The investigation of other targets like Ni and Cu in Group 2 reveals that calculations using Bertini–Jülich give cross sections lying closest to the experimental results.

Fig. 3 shows experimental and INC-calculated helium cross sections for Ag in Group 3, the intermediate-weighted targets. Reasonable agreement is found between Bertini–GCCI or HETC and the experimental cross sections. For proton energies below 1 GeV, the experimental data fall on the HETC/GCCI curve with MPM off. Above 1 GeV, the experimental data are closer to HETC/GCCI-calculated data with MPM on. But in the whole energy range, Bertini–HETC/GCCI agrees better with MPM off than with MPM on. It has to be reminded that the curves for Bertini–HETC and Bertini–GCCI lie so close to one another, it is difficult to decide which model is the better choice for Group 3 targets.

Figs. 4 and 5 show the same kind of information for heavy targets Pb and U, respectively. In Group 4, Pb and also W, Hg, and Bi are common target materials in spallation facilities. U is categorized in a separate group due to its fission ability. As observed in Figs. 4 and 5, for heavy targets CEM2k results show a nice agreement with the experimental data. The Bertini model clearly overestimates helium production.

Current tentative recommendations for calculation of helium cross sections may be summarized as in Table 2. For light and intermediate-weighted targets (Groups 1–3), the Bertini model shows the closest agreement to the experimental data though the level density has to be carefully configured for materials in the different groups. For heavy targets (Groups 4 and 5), CEM2k gives closest agreement.

Table 2
Tentative recommendations for calculation of proton-induced helium cross sections

	$E < 150$ MeV	$150 < E < 3200$ MeV
Groups 1 and 2	LA150[a]	Bertini–Jülich
Groups 3	LA150[a]	Bertini–HETC/GCCI–MPM off
Groups 4 and 5	LA150[a]	CEM2k

[a] LA150 when available; otherwise same as for $150 < E < 3200$ MeV.

4. Neutron-induced helium cross sections

The neutron-induced helium cross sections at high energies are calculated in the same way as discussed above for the proton-induced helium cross sections. However, due to the difficulty in producing monoenergetic neutrons at high energies, there are nearly no experimental data to benchmark the INC-calculated neutron-induced helium cross sections. But for high-energy protons, Coulomb interactions have only a slight effect on spallation reactions. Therefore, the neutron-induced helium cross section at a given energy can be estimated to be approximately the same as the proton-induced cross section. Fig. 6 shows the ratios of neutron- to proton-induced helium cross sections for Al, Fe and W. The cross sections are calculated using the same INC model with the same level-density option for each material. For particle energies above 500 MeV, we see in Fig. 6 that the neutron- and proton-induced cross sections are nearly equal. Therefore, the recommended calculation codes and sources for neutron-induced helium cross sections can be taken from Table 2, where the corresponding proton cross section recommendations are summarized.

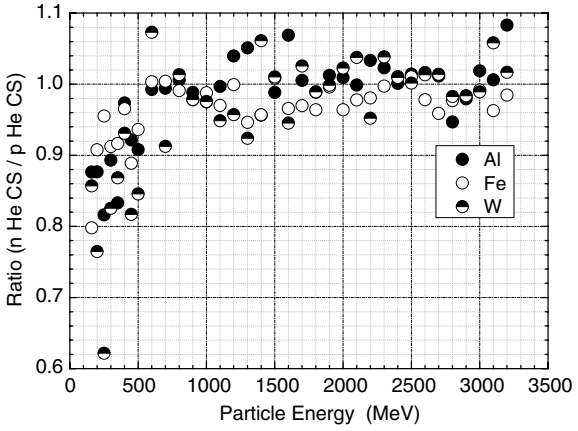

Fig. 6. Ratios of neutron-induced to proton-induced helium cross section versus particle energy for Al, Fe and W (calculated by Bertini–Jülich with MPM on for Al and Fe and CEM2k for W).

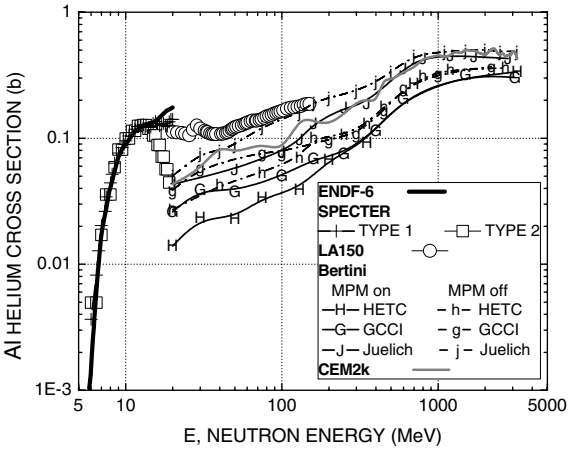

Fig. 7. Helium cross section versus neutron energy for Al. High-energy calculations and low-energy calculations (LA150, ENDF-6 and SPECTER).

For energies below 20 MeV, there are more calculated cross section data available for neutrons (from ENDF-6, SPECTER, and LA150) than for protons (provided only by LA150). Fig. 7 shows the low-energy and high-energy cross sections for neutrons on Al. Below 20 MeV, SPECTER has two types of cross sections, as discussed by Charlton et al. [40] and designated as Type 1 and Type 2. SPECTER-Type 2 does not take into account the (n, xn) channels for helium production where $x > 1$. SPECTER-Type 1, however, includes all the He produced and is usually the more relevant quantity. As can be seen in Fig. 7, the SPECTER-Type 1 cross sections agree well with ENDF-6 values, and they make a better match with LA150 values at 150 MeV.

5. Summary

The NCSU radiation damage database is described. The Database contains damage energy, displacement, helium, and hydrogen cross sections for 23 elemental targets and 8 alloys for proton and neutron energies up to 3.2 GeV. In this paper, our attention is concentrated on cross sections for the production of helium mainly by protons, but it is shown that above 500 MeV the neutron and proton cross section values are quite similar. The high-energy INC calculations are benchmarked with the available experimental data. The results show that the Bertini model is good for estimating helium production for light and intermediate-weighted targets, but overestimates the cross sections for heavy targets. Even for light and intermediate-weighted targets, a proper level-density model has to be carefully chosen when using Bertini model. CEM2k, on the other hand, is in fair agreement with experiment for heavy targets, but gives underestimates for low and intermediate-weighted targets. In general, it must be said that, based on the type of information presented (Figs. 1–5), recommendations as to which codes and which options within the codes give best agreement with experiment are somewhat uncertain. In order to achieve more reliable cross section calculations for particular targets and energy ranges, there needs to be available a wider body of well-based experimental and calculated information concerning helium production in spallation-irradiated materials.

References

[1] M.S. Wechsler, J.F. Stubbins, W.F. Sommer, P.D. Ferguson, E.H. Farnum, Selection and Qualification of Materials for the Accelerator Transmutation of Waste Project, LA-UR-92-1211, Los Alamos National Laboratory, Los Alamos, NM, 1992.

[2] W. Lu, M.S. Wechsler, P.D. Ferguson, E.J. Pitcher, in: Proceedings, Twelfth International Symposium on Reactor Dosimetry, Gatlinburg, Tennessee, USA, May 2005, J. ASTM Int. 3 (7) (2006). www.astm.org, Paper ID JAI13467.

[3] W. Lu, M.S. Wechsler, Y. Dai, in: Proceedings, Seventh International Workshop on Spallation Material Technology, Thun, Switzerland, June 2005, J. Nucl. Mater. 306 (2006) 280.

[4] H.W. Bertini, Phys. Rev. 131 (1963) 1801.

[5] H.W. Bertini, Phys. Rev. 188 (1969) 1711.

[6] R.E. Prael, H. Lichtenstein, User Guide to LCS: The LAHET Code System, Report LA-UR-89-3014, Los Alamos National Laboratory, Los Alamos, New Mexico, 1989.

[7] S.G. Mashnik, A.J. Sierk, O. Bersillon, T. Gabriel, Nucl. Instrum. and Meth. A 414 (1998) 68. Also, Report LA-UR-97-2905, Los Alamos National Laboratory, Los Alamos, NM, 1997.

[8] S.G. Mashnik, A.J. Sierk, in: Proceedings of 2000 ANS/ENS International Meeting, Nuclear Applications of Accelerator Technology (AccApp00), Washington DC, USA, 12–16 November 2000.

[9] L.R. Greenwood, R.K. Smither, SPECTER: Neutron Damage Calculations for Materials Irradiations, ANL/FPP/TM-197, Argonne National Laboratory, Argonne, Illinois, 1985, 60439.

[10] V. McLane, (Ed.), ENDF-102, Data formats and procedures for the evaluated nuclear data file ENDF-6, BNL-NCS-44945-01/04-Rev., National Nuclear Data Center, Brookhaven National Laboratory, Upton, New York, 2001.

[11] M.B. Chadwick, P.G. Young, S. Chiba, S.C. Frankle, G.M. Hale, H.G. Hughes, A.J. Koning, R.C. Little, R.E. MacFarlane, R.E. Prael, L.S. Waters, Nucl. Sci. Eng. 131 (1999)

293, see also, LA-UR-98-1825, Los Alamos National Laboratory, 1998.
[12] J.F. Ziegler, J.P. Biersack, U. Littmark, The Stopping and Range of Ions in Solids, Pergamon, New York, 1985, see also, www.srim.org.
[13] A. Gilbert, A.G.W. Cameron, Can. J. Phys. 43 (1965) 1446.
[14] J.L. Cook, H. Ferguson, A.R. deL. Musgrove, Aust. J. Phys. 20 (1967) 477.
[15] A.V. Ignatyuk, G.N. Smirenkin, A.S. Tishin, Sov. J. Nucl. Phys. 21 (1975) 55.
[16] K.C. Chandler, T.W. Armstrong, Operating Instructions for the High-Energy Nucleon–Meson Transport Code HETC, ORNL-4744, Oak Ridge National Laboratory, Oak Ridge, Tennessee, 1972.
[17] P. Cloth, D. Filges, G. Sterzenbach, T.W. Armstrong, B.L. Colborn, The KFA-version of the high-energy transport code HETC and the generalized evaluation code SIMPEL, Jül-Spez-196, Kernforschungsanlage Jülich GmbH, 1983.
[18] L.S., Waters, MCNPX User's Manual, Version 2.3.0, Report LA-UR-02-2607, Los Alamos National Laboratory, Los Alamos, New Mexico, 2002.
[19] Y. Dai, Y. Foucher, M.R. James, B.M. Oliver, J. Nucl. Mater. 318 (2003) 167.
[20] O.A. Schaeffer, J. Zahringer, Phys. Rev. 113 (1959) 674.
[21] R.H. Bieri, W. Schultes, Helvetica Physica Acta (1962) 553.
[22] K. Goebel, H. Schultes, J. Zahringer, Report CERN 64 (12) (1964).
[23] S.L. Green, W.V. Green, F.H. Hegedus, M. Victoria, W.F. Sommer, B.M. Oliver, J. Nucl. Mater. 155–157 (1988) 1350.
[24] R. Michel, M. Gloris, H.-J. Lange, I. Leya, M. Lupke, U. Herpers, B. Dittrich-Hannen, R. Rosel, Th. Schiekel, D. Filges, P. Dragovitsch, M. Suter, H.-J. Hofmann, W. Wolfli, P.W. Kubik, H. Baur, R. Wieler, Nucl. Instr. Meth. B 103 (1995) 183.
[25] B.M. Oliver, M.R. James, F.A. Garner, S.A. Maloy, J. Nucl. Mater. 307–311 (2002) 1471.
[26] B. Dittrich, U. Herpers, R. Bodemann, M. Lupke, R. Michel, P. Signer, R. Wieler, H. Hofmann, W. Woelfli, Nucl. Energy Agency Nucl. Data Committee Rep. (E)-312-U (1990) 53.
[27] J.P. Alard, A. Baldit, R. Brun, J.P. Costilhes, J. Dhermain, J. Fargeix, L. Fraysse, J. Pellet, G. Roche, J.C. Tamain, Nuovo Cimento A30 (1975) 320.
[28] R. Michel, F. Peiffer, S. Theis, F. Begemann, H. Weber, P. Signer, R. Wieler, P. Cloth, P. Dragovitsch, D. Filges, P. Englert, Nucl. Instrum. and Meth. B 42 (1989) 76.
[29] I. Leya, H. Busemann, H. Baur, R. Wieler, M. Gloris, S. Neumann, R. Michel, F. Sudbrock, U. Herpers, Nucl. Instrum. and Meth. B 145 (1998) 449.
[30] H. Dubost, B. Gatty, M. Lefort, J. Peter, X. Tarrago, Journal De Physique 28 (1967) 257.
[31] K. Goebel, H. Schultes, J. Zahringer, Report CERN 64 (1964) 12.
[32] E.K. Hyde, G.W. Butler, A.M. Poskanzer, Phys. Rev. C 4 (1971) 1759.
[33] F.A. Garner, B.M. Oliver, L.R. Greenwood, M.R. James, P.D. Ferguson, S.A. Maloy, W.F. Sommer, J. Nucl. Mater. 296 (2001) 66.
[34] R.E.L. Green, R.G. Korteling, Phys. Rev. C 22 (1980) 1594.
[35] E.N. Volnin, G.M. Amalsky, D.M. Seleverstov, N.N. Smirnov, A.A. Vorobyov, Phys. Lett. B 55 (1975) 409.
[36] A.M. Poskanzer, G.W. Butler, E.K. Hyde, Phys. Rev. C 3 (1971) 882.
[37] D. Hilscher, C.M. Herbach, U. Jahnke, V. Tischenko, M. Enke, D. Filges, F. Goldenbaum, R.D. Neef, K. Nuenighoff, N. Paul, H. Schaal, G. Sterzenbach, A. Letourneau, A. Böhm, J. Galin, B. Lott, A. Péghaire, L. Pienkowski, J. Nucl. Mater. 296 (2001) 83.
[38] M. Enke, C.M. Herbach, D. Hilscher, U. Jahnke, O. Schapiro, A. Letourneau, J. Galin, F. Goldenbaum, B. Lott, A. Péghaire, D. Filges, R.D. Neef, K. Nünighoff, N. Paul, H. Schaal, G. Sterzenbach, A. Tietze, L. Pienkowski, Nucl. Phys. A 657 (1999) 317.
[39] National Spallation Neutron Source Conceptual Design Report, NSNS/CDR-2/VI, Oak Ridge National Laboratory, Oak Ridge, TN 37831, 1997.
[40] L.A. Charlton, L.K. Mansur, M.H. Barnett, R.K. Corzine, D.J. Dudziak, M.S. Wechsler, in: Proceedings of the Second International Topical Meeting on Nuclear Applications of Accelerator Technology (AccApp'98), American Nuclear Society, La Grange Park, Illinois 60526, 1998, p. 247.